JOURNAL OF MATERIALS SCIENCE **34** (1999) 3367–3374

Thermal stability of zirconia membranes

LI SHI, KAM-CHUNG TIN, NING-BEW WONG*
Department of Biology and Chemistry, City University of Hong Kong, Hong Kong
E-mail: bhnbwong@cityu.edu.hk

Yttria-doped zirconia and pure zirconia membranes were prepared with sol-gel method using zirconium oxychloride octahydrate ($ZrOCl_2 \cdot 8H_2O$) as starting material. Characterization for membranes was performed by means of BET, TG-DTA, SEM, XRD, FT-IR and Raman spectroscopy. Stable tetragonal phase and pore structure in yttria-doped zirconia membranes were observed at 400–700 °C. And, phase transformation temperature can be retarded to 300 °C. As a result, yttria doping can be developed as a method to secure the membrane from cracking in preparation process and high temperature applications.

1. Introduction

Zirconia membranes are known to be chemically more stable than titania and γ-alumina membranes, and therefore are more suitable for applications in liquid phase under harsh condition [1]. Since zirconia is one of the common catalysts, it is a potential membrane material for high temperature catalytic reactions [2]. Sol-gel method has been shown to be most practical in fabrication of porous ceramic membranes. Techniques in coating pure ZrO_2 [3–5] and Y_2O_3-doped ZrO_2 [6–8] prepared by sol-gel method have been investigated for many years because of several advantages such as low processing temperatures, homogeneity, crack-free coating and low cost. Sol-gel derived zirconia membranes are normally in the metastable tetragonal phase while those prepared from other methods are in monoclinic phase [9]. At temperatures higher than 400 °C, the tetragonal phase of zirconia transforms to stable monoclinic phase. Along with the transformation, crack usually results in the membrane layer due to change of lattice dimension and stress developed in the membrane [10, 11]. For high temperature application, it is important to stabilize the phase structure of zirconia. It was reported that a thermally stable phase structure of zirconia was observed in an yttria-doped zirconia membrane [12]. However, there is lack of study on the thermal stability of zirconia membranes prepared by sol-gel method.

Sol-gel membranes of zirconia are conventionally made with metal alkoxides [13–15], while little attention has been paid to the method of preparing stabilized sol with non-alkoxides as starting materials. Systematic study on thermal stability of doped and pure zirconia membranes is still rare.

In this work, $ZrOCl_2 \cdot 8H_2O$, yttria and PVA were used as starting material, dopant and binder, respectively, to prepare yttria-doped zirconia membranes by sol-gel method. Characterization and stability of membranes were determined via thermal analysis, phase analysis, Raman and IR spectroscopy.

2. Experimental

Sol-gel technique used to prepare a supported or unsupported inorganic membrane includes the following steps: synthesis of stable sol; mixing zirconia sol with dopant and organic binder solutions; making unsupported and supported membrane; drying and calcination the membrane. Preparation of stable zirconia sol was reported as a more difficult process as compared with other sols such as boehmite and titania [10] because of the extremely rapid reaction of the zirconia alkoxide with water. This makes the synthesis of the zirconia sol very sensitive to experimental conditions and requires extreme carefulness. To avoid the above difficulties, an alternative way is to use $ZrOCl_2 \cdot 8H_2O$ as starting material to prepare zirconia oxalate sol, which is in turn converted to zirconia sol.

Zirconyl oxalate sol was prepared from reacting the $ZrOCl_2 \cdot 8H_2O$ (Fluka) with $H_2C_2O_4 \cdot 2H_2O$ (Acros) in aqueous solution. Solutions of 0.25 M $H_2C_2O_4$ and 0.5 M $ZrOCl_2$ in 2 : 1 volume ratio were mixed at room temperature with gentle stirring. A white sol was developed at 50 °C. These sol particles are mainly hydrated zirconyl oxalate ($ZrOC_2O_4$) peptized by HCl which is one of the products of the above reaction.

Solutions of 0.24 M yttrium nitrate, $Y(NO_3)_3$ (Acros), and 1.40 mM PVA (Fluka, MW = 72000) were prepared by dissolving the chemicals in 100 ml water. Desired amount of PVA solution was added to the sol. After 2 h stirring and 1 h setting, the sol was ready to be used for coating. The PVA was used as organic binder to prevent forming crack in drying process.

The yttrium nitrate solution was mixed with the stable zirconia sol at room temperature in a desired proportion to make 3 mol % yttria-doped zirconia by a solution-sol mixing method.

* Author to whom all correspondence should be addressed.

Mixing of $Y(NO_3)_3$ with the organic binder (PVA) to the zirconia sol should be carefully handled since stability of the sol is quite sensitive to pH, ion concentration and other conditions. Insufficient amount of PVA can introduce cracks in the membrane, while excessive amount may cause swelling.

Unsupported membrane was prepared by pouring the sol into a petri-dish, and supported membrane was made by dip coating the sol on a pre-polished U type tubular porous ceramic support. The outer diameter and thickness of the supporting tube are 5 and 0.5 cm, respectively. This configuration can ensure good mechanical properties of the membrane. The outer part of the tubular support was coated with sol by dip coating. The thickness of a singly coated zirconia layer after firing treatment should be less than 2 μm, since thicker membrane may cause more defects. Therefore, low zirconia concentration in the sol and sufficient amount of organic binder are required for preparation.

Each coating was proceeded by dipping ceramic support tube into the sol for 10 s. After dip coating, dish and support were dried at room temperature and 60% relative humidity for at least 12 h. The coating layer was then fired at 50 °C/h to a desired temperature for 2 h, and the membrane was ready for use or characterization. For supported membrane, this coating process was repeated until a desired thickness is obtained.

Pore size, surface area, pore volume and pore size distribution of the unsupported membranes were measured from nitrogen ad(de)sorption isotherms by means of an adsorption porosimeter (Micrometrics, NOVO 1000). A D/max-3c type X-ray diffractometer (Rigaku) was used to identify the phase structures using CuK_α radiation at a scanning rate of 4° min^{-1}. Fourier transform infrared spectroscopy (FT-IR system 1600, Perkin-Elmer Co.) was used to identify the vibrational features of the zirconia. IR spectra were recorded from 4000 to 200 cm^{-1}. Concentrations of zirconia of all sample pellets used for FT-IR measurement are 1 wt % in KBr. Raman spectroscopy was also used as a complementary tool for characterization. Thickness of the film was determined by scanning electron microscopy (SEM) on the fractured surface of a membrane.

Characterization for membranes formation was achieved by thermogravimetric-differential thermal analysis (Seiko). Samples of unsupported membranes dried at 10 °C/min^{-1} were used for thermal analysis.

3. Results and discussion

3.1. Pore structural of membranes

The pose size distributions (PSD) of pure and yttria-doped zirconia membranes after calcination and sintering at different temperatures are shown in Figs 1 and 2. In Fig. 1, the PSD of pure membranes after calcination at 400 °C is rather narrow. But, after further heat treatment, the PSD spreads out and the pore size increases. At 300–400 °C, zirconia decomposes, zirconia metastable tetragonal phase starts to appear, and rearrangement in pore structure takes place along with crystallization. After heat treatment at 400 °C, some monoclinic phase is transformed from tetragonal phase, and this results in pore size increasing.

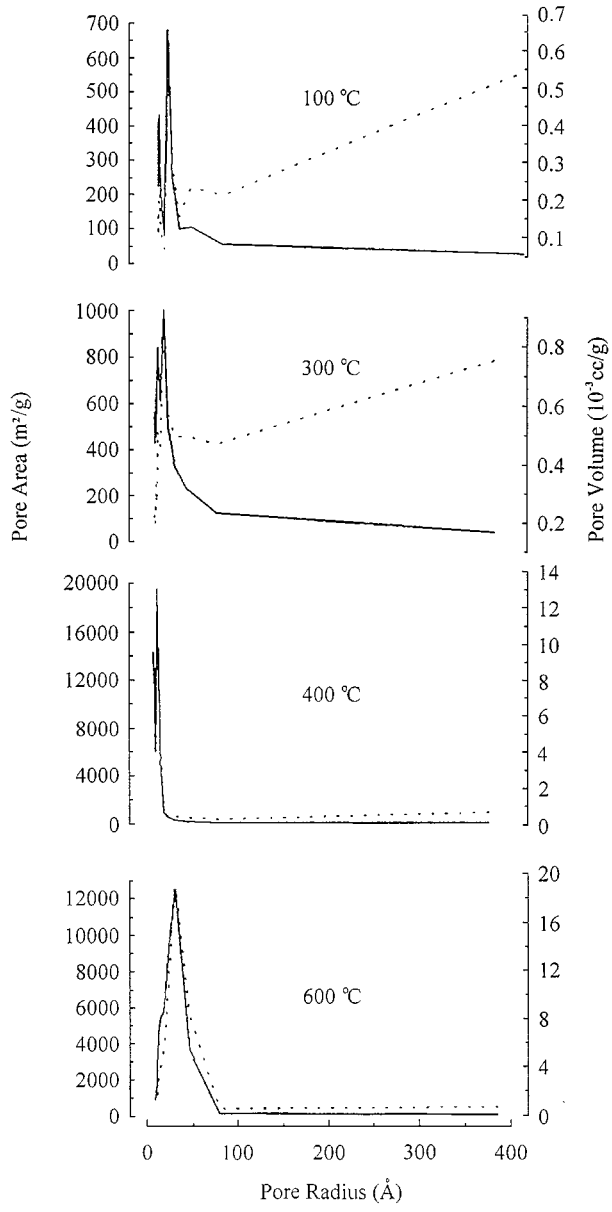

Figure 1 The pore size distributions of pure zirconia membranes at different temperatures.

As the tetragonal phase of yttria-doped zirconia membrane formed at 400 °C, from the pore volume data in Fig. 2, it can be seen that their PSDs are almost unchanged at 400–600 °C since no phase transformation occurred. Above 700 °C, number of larger size pore increases due to particle sintering [16, 17]. After sintering, the surface area decreases, and the pore volume of the membrane also decreases. This is consistent with theoretical predictions.

After calcination at 400 °C for 2 h, the average pore size in pure zirconia membrane is 2.1 nm, which is much smaller than that (5.0 nm) in the yttria-doped one. The BET surface areas of pure and doped membranes are 71.3 and 50.58 m^2/g, respectively. After heat treatment at 600 °C, the pore size of pure and yttria-doped zirconia change to 6.0 and 5.3 nm, respectively, and the surface areas of pure and yttria-doped zirconia change to 30.5 and 47.103 m^2/g. For comparison, the pore size and surface areas of the two types of membranes are listed in Table I.

TABLE I The comparison of pore size and surface area after heat treatment

	400 °C		600 °C		% Change	
	D^a	A^b	D	A	D	A
Pure ZrO_2	2.1 nm	71.3 m^2/g	6.0 nm	30.5 m^2/g	186	57.2
Yttria-doped ZrO_2	5.0 nm	50.6 m^2/g	5.3 nm	47.1 m^2/g	6	6.9

[a]Pore diameter.
[b]Surface area.

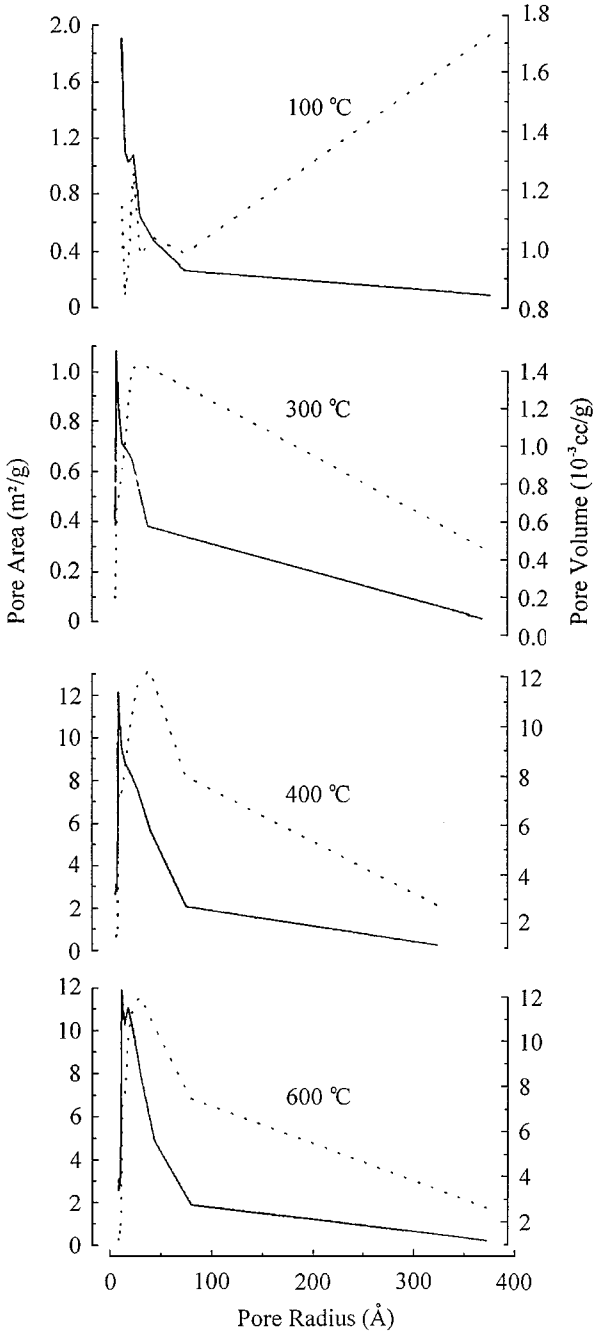

Figure 2 The pore size distributions of yttria-doped zirconia membranes at different temperatures.

3.2. Thermal properties of membranes

Figs 3 and 4 show TG and DTA curves for pure zirconia and 3 mol % yttria doped zirconia gel. They are prepared from the coating solution dried at 100 °C for 12 h. Endothermic and exothermic peaks were observed in weight loss region below 500 °C, and no other thermal effect was observed above this temperature. The origin of weight loss is attributed to the dehydration and decomposition of oxalate compounds.

In Fig. 3, thermal decomposition of the zirconyl oxalate gel presents two types of mass losses: (1) dehydration below 250 °C corresponding to $ZrOC_2O_4 \cdot xH_2O \rightarrow ZrOC_2O_4 + xH_2O$; (2) decomposition at 250–400 °C according to $ZrOC_2O_4 \rightarrow ZrO + 2CO_2$. The release of chlorine takes place slowly during the entire thermal treatment process, and there is an increased loss at 480 °C due to crystallization of zirconia.

Dried samples containing 3 mol % Y_2O_3 exhibit similar DTA curves as shown in Fig. 4. An exothermic peak at around 480 °C can also be attributed to the crystallization of zirconia. But this peak is weaker than that of pure zirconia because of the slower crystallization process in yttria-doped zirconia. Its crystal is composed of a stable tetragonal phase. For pure zirconia, the transformation rate of the tetragonal phase to the monoclinic phase is much faster than the formation rate of the tetragonal phase. Therefore, the tetragonal phase is only a metastable phase or a transition state and will not be accumulated during the crystallization process. Ramanathan *et al.* [18] accounted the sharp exothermic DSC peak to the drastically reduced crystallization of zirconia by increase of yttria content. As shown in Fig. 3, the exothermic peak includes crystal formation and phase transformation. This was also confirmed by the XRD data. On the endothermic peak, there is a small shoulder, which indicates the decomposition of yttria oxalate. The transformation from tetragonal phase to monoclinic phase is a second order phase, which is an intrinsically slow process, and there in no other thermal effect observed above 500 °C.

3.3. Phase structure of membranes

X-ray power diffraction was used to characterize the zirconyl oxalate gel and its membranes. As shown in Figs 5 and 6, amorphous structures of both pure and yttria doped zirconias were observed below 300 °C.

Fig. 5 shows X-ray diffraction patterns of pure ZrO_2 membranes obtained from different thermal treatments. In the figure, the first two diffractograms correspond to the as-prepared and 300 °C heated zirconia which are essentially amorphous. When the zirconia gel is heated to 400 °C, some broad lines develop which correspond to the crystallization of tetragonal zirconia. The t and m denote the tetragonal and the monoclinic phases, respectively. Near the main peak (111 plane) of tetragonal phase there is a very weak peak of monoclinic phase. As the temperature raises, the monoclinic phase increases rapidly on the expense of the tetragonal phase. At

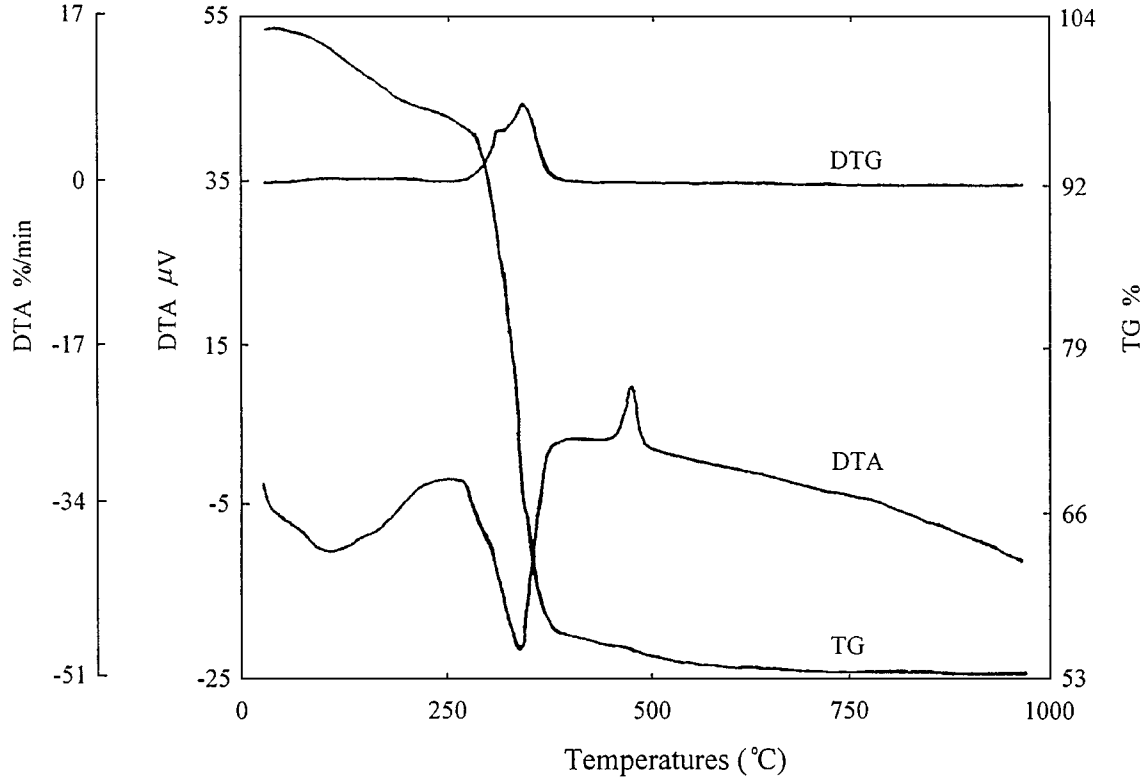

Figure 3 TG and DTA curves for the pure zirconia sample.

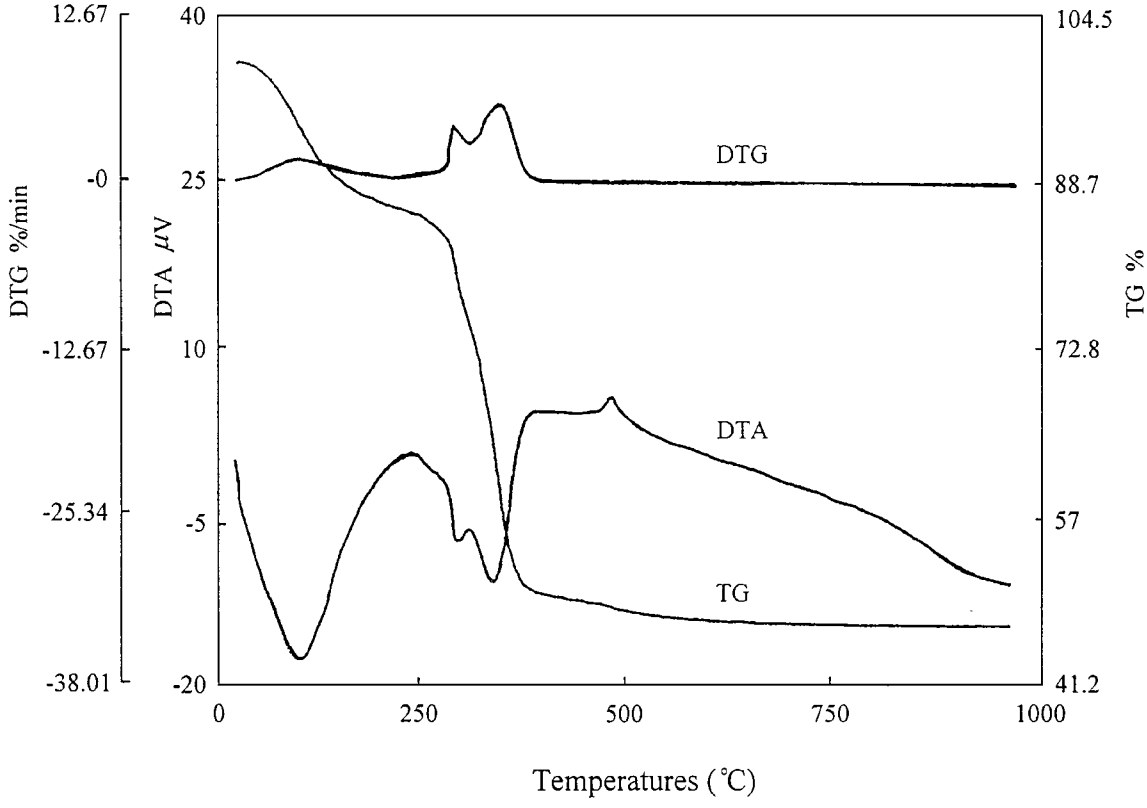

Figure 4 TG and DTA curves for the yttria-doped zirconia sample.

800 °C, crystallized monoclinic zirconia is well established. At 1000 °C, the major component is the monoclinic zirconia with a tiny amount of tetragonal phase left. The steady progression of phase transition is monitored with progressive heating.

The peak height ratio of $(111)_T$ to $[(111)_M + (111)_T]$ was used to estimate the fraction of the tetragonal phase present in the sample. For sample, the fraction of tetragonal phase in a sample was 0.21 after heat treatment at 900 °C, and 0.08 at 1000 °C.

Fig. 6 is the XRD pattern of an yttria doped zirconia sample containing stable tetragonal phase at 400–700 °C. It is known that for zirconia with small crystallite size, metastable tetragonal phase exists at low

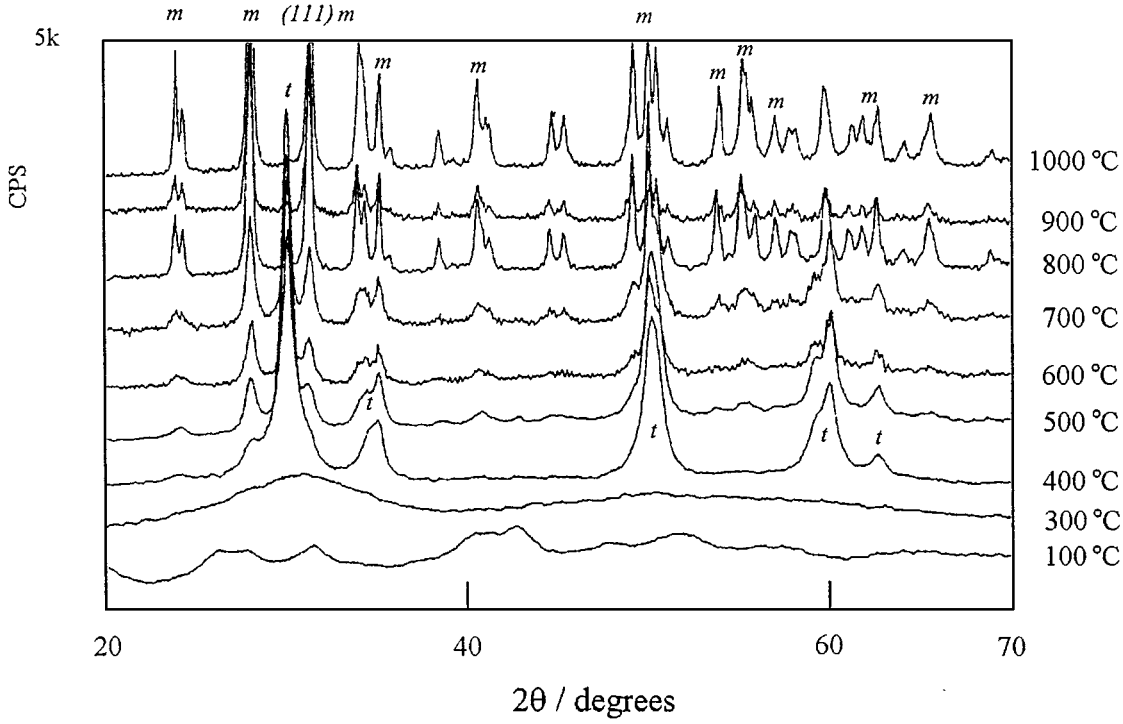

Figure 5 XRD patterns of pure zirconia membranes after heat treatment at different temperatures.

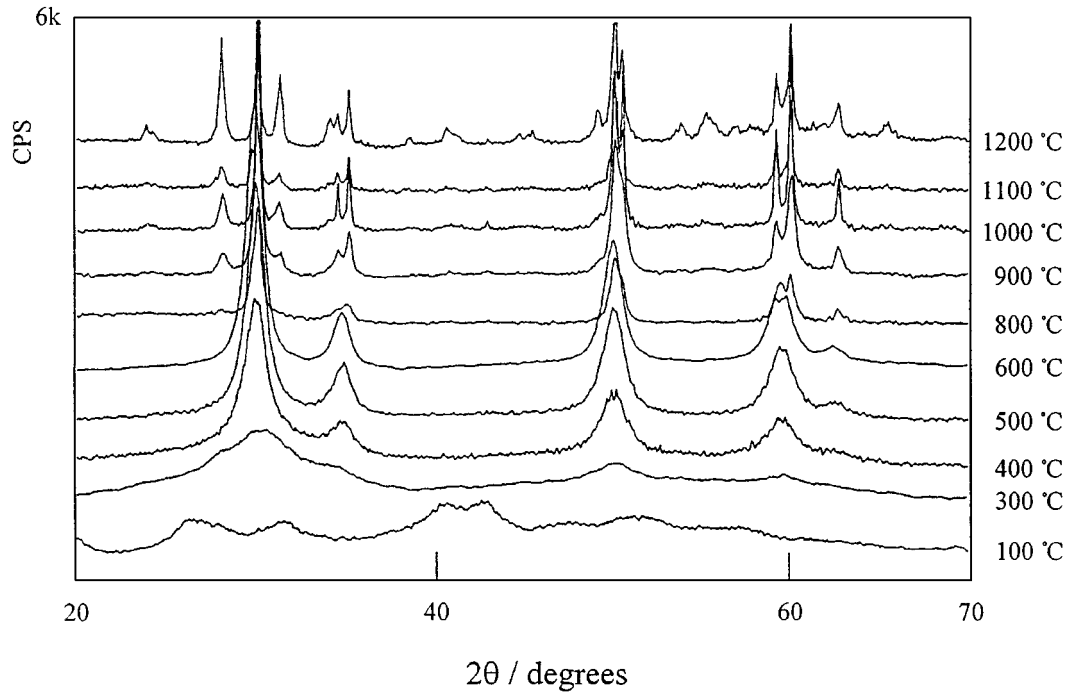

Figure 6 XRD patterns of yttria-doped zirconia membranes after heat treatment at different temperatures.

temperatures as a result of the crystallite size effect [19]. Crystallite sizes of membranes obtained in this study are smaller than 25 nm, which is the critical value of the crystallite size effect. This behaviour in crystallization is strongly affected by the yttria dopant. It was showed that activation energy and temperature of the phase transformation from tetragonal to monoclinic both increased with the amount of yttria doped.

Variation of crystallite with heat-treatment temperature was estimated from X-ray diffraction line broadening (XRD-LB) measurements. Scherrer equation [20] $D = k\lambda / B \cos \vartheta$ was used for the calculation, where D is the crystallite size (nm), ϑ is the Bragg angle (deg), k is a constant which equals to 0.89, and B is the calibrated width of a diffraction peak at half-maximum intensity.

At 800 °C, phase transformation occurs, but the fraction of monoclinic phase in zirconia is only 0.27 even at 1200 °C. Therefore, yttria can retard phase transformation and decrease the rate of transformation.

The crystallite size increases with increasing heat-treatment temperature, and saturates at 1200 °C. This

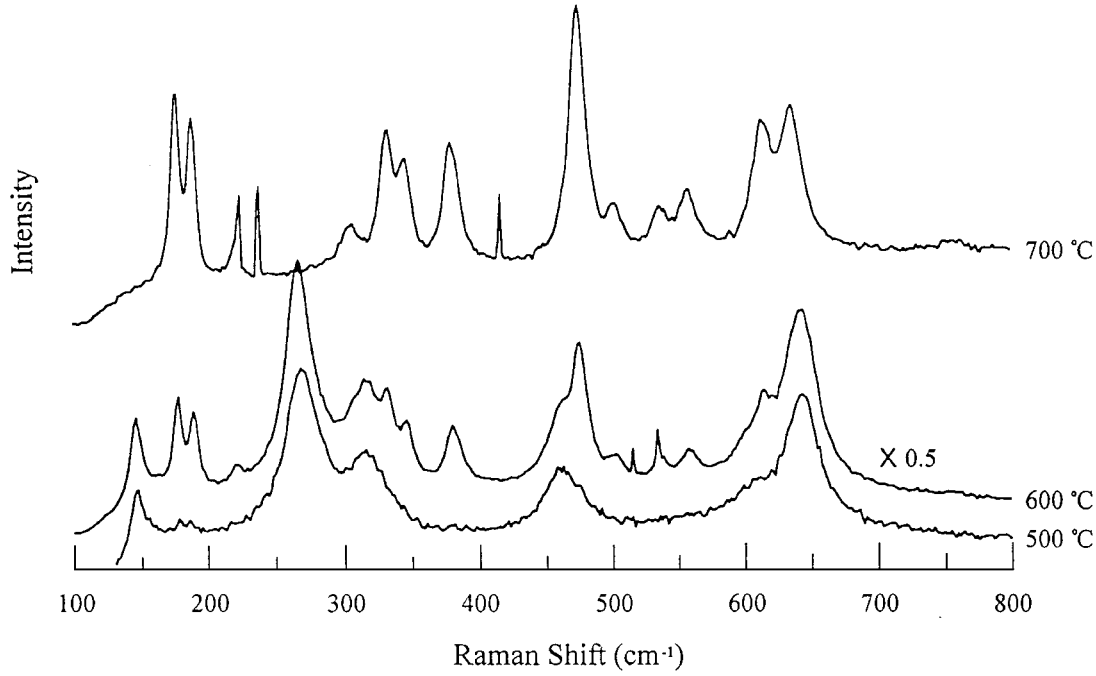

Figure 7 Raman spectra of zirconia membranes at different treatment temperatures.

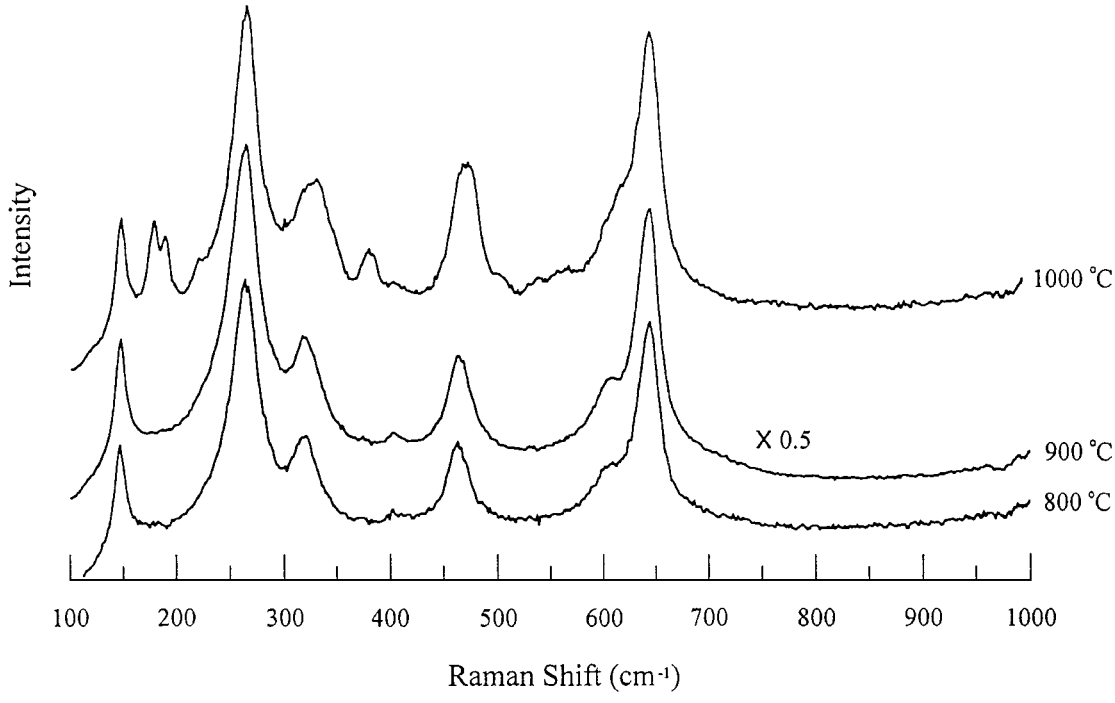

Figure 8 Raman spectra of yttria-doped zirconia membranes at different treatment temperatures.

indicates that the growth of crystals in the film ceases at 1200 °C. This may be attributed to the suppression of crystallization by the existence of yttria.

Figs 7 and 8 are Raman spectra of pure and yttria-doped zirconia membranes at different temperatures. A different number of Raman bands for the tetragonal and cubic (fluorite) structures of pure zirconia was predicted by means of factor group analysis. Tetragonal ZrO_2 belongs to the $P4_2/nmc$ space group (D_{4h}^{15}) with two molecules per unit cell and therefore six vibrational modes ($A_{1g} + 2B_{1g} + 3E_g$) are Raman active. Monoclinic zirconia belongs to monoclinic $P2_1/b$ (C_{2h}^5) space group with four molecules per unit cell. 18 Raman active vibrational modes ($9A_g + 9B_g$) are predicted [21]. Among them 14 bands are observed at room temperature, and their positions are in accordance with other's work. This suggests that the crystal is monoclinic in a zirconia membrane.

Fig. 7 exhibits the Raman spectra of ZrO_2 at some selected temperatures. The ZrO spectrum at 500 °C corresponds to the tetragonal phase. The assignment of the Raman-active modes ($A_{1g} + 2B_{1g} + 3E_g$) for the t-phase are: B_{1g} at 147 cm^{-1}, E_g at 269 cm^{-1}, B_{1g} at 315 cm^{-1}, E_g at 459 cm^{-1}, A_{1g} at 600 cm^{-1} (very weak) and E_g at 643 cm^{-1}. For spectrum obtained below 500 °C, none of the lines can be assigned to the

m-phase. This is in agreement with our previous XRD study that only traces of the m-phase in pure zirconia exist below 500 °C, and the amount of the m-phase gradually increases with increasing temperature.

As the temperature is increased, Raman-active modes of the t-phase change in their frequency, linewidth and intensity. The Raman-active modes of the m-phase appear at 600 °C are assigned to A_g at 176 and 187 cm^{-1}, B_g at 220 cm^{-1}, A_g at 300 cm^{-1}, B_g at 333, 344 and 380 cm^{-1}, A_g at 475 cm^{-1}, B_g at 510 and 536 cm^{-1}, A_g at 558 cm^{-1}, B_g at 613 cm^{-1}, A_g at 635 and 760 cm^{-1}. At 700 °C, all Raman-active modes ($A_{1g} + 2B_{1g} + 3E_g$) for the t-phase are not observed and only those of the m-phase appear. For yttria-doped zirconia sintered at 1000 °C in the present work, no Raman-active modes for the m-phase can be observed before the t-m phase transition because of its martensitic character. In addition, both the A_g modes at 176 and 187 cm^{-1} are not fully resolved, and the 329 cm^{-1} B_g mode is also not resolvable from the A_g mode at ~334 cm^{-1}.

In monoclinic ZrO_2, each Zr atom is surrounded by seven oxygen atoms with the Zr-O distances between 2.05 and 2.27 (average 2.159), whereas in tetragonal ZrO_2, each Zr atom is surrounded by eight oxygen atoms with unequal Zr-O distances (four at 2.10 and the others at 2.35; average 2.226) [22, 23]. Assuming that similar Zr-O distances exist in both phases in yrrria doped zirconia, the shift from the 315 cm^{-1} (B_{1g}) and the 459 cm^{-1} (E_g) of the t-phase to the 333 cm^{-1} (B_g) and 475 cm^{-1} (A_g) of the m-phase correspond to atomic displacements in the course of the t-m phase transition. Same explanation can be made to the shift from the 600 cm^{-1} (A_{1g}) to the 613 cm^{-1} (B_g) at 700 °C. This result is in agreement with that of Hirata [22].

At 700 °C, the Raman line shifts from 643 to 635 cm^{-1} as it results from the transformation of E_g mode of t-phase into A_g mode of m-phase. This may be complicate to explain the Raman shift only from the variation in Zr-O distances.

Actually, lattice parameters of the monoclinic ZrO_2 ($a = 5.142$, $b = 5.206$, $c = 5.313$ and $\beta = 99.18°$) [23, 24] are different from those of the tetragonal ZrO_2 ($a = 5.222$ and $c = 5.212$) [25, 26], and this accounts for the different Zr-O distances between the two phases. However, it is difficult to tell whether the shift of Raman frequency from 643 cm^{-1} (E_g, t-phase) to 635 cm^{-1} (A_g, m-phase) is correlated to the different Zr-O distances in the two phases. During the t-m phase transition, the atomic arrangement changes significantly. This results in a change in force constants and eventually a change of Raman frequency.

FT-IR spectra of zirconia is shown in Fig. 9. There is a broad Reststrahlen band of t-phase around 480 cm^{-1} at lower temperature. As temperature increases, it gradually splits to five bands corresponding to the m-phase. These five peaks (358, 420, 500, 576, and 742 cm^{-1}) are much intensified at 800 °C. On the other hand, there is still a broad Reststrahlen band at 800 °C. The trace of characteristic peak of m-phase at 900 °C is in good agreement with the XRD results. From 300 to 400 °C, the oxalate ligand decomposes rapidly and is indicated by the carbonyl peak of υ_{as}(C=O) at 1680 cm^{-1}. These observations are consistent with the thermal analysis results.

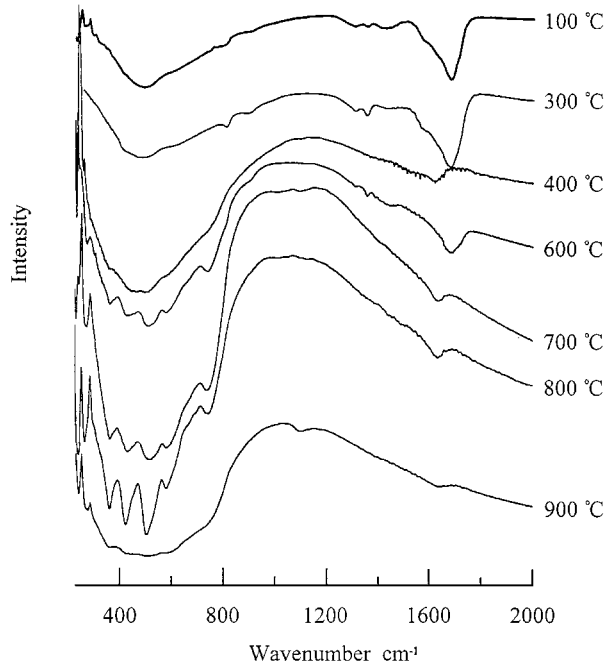

Figure 9 IR spectra of pure zirconia membranes.

4. Conclusions

In this work, zirconium chloride octahydrate has been demonstrated as a good starting material for preparation of stable zirconia sol. Uniformly thin membranes of pure and yttria-doped zirconias were successfully fabricated by slip-doping with sol-gel method.

In both pure and yttria-doped zirconia membranes, amorphous phase exists below 300 °C and tetragonal phase appears at 400 °C. At 400–600 °C, an unstable monoclinic phase is formed in pure zirconia, and further transforms to a stable tetragonal phase with pore structure in yttria-doped zirconia. The phase transformation temperature can be retarded to 300 °C by yttria-doping in the zirconia membranes.

None of the Raman-active modes ($9A_g + 9B_g$) of the m-phase are detected prior to the t-m phase transition, while all Raman active modes ($A_{1g} + 2B_{1g} + 3E_g$) of the t-phase are observed.

Acknowledgements

L. Shi would like to acknowledge the Research Studentship Award from the City University of Hong Kong.

References

1. R. R. BHAVE, "Inorganic Membranes, Synthesis, Characterization and Properties" (Van Rostrnd Reinhold, New York, 1991).
2. H. P. HSIEH, *Inorganic Membranes, A. I. Ch.E. Symp. Ser.* **84** (261) (1998) 1.
3. L. YANG and J. CHENG, *J. Non-Cryst. Solids* **112** (1989).
4. K. IZUMI, M. MURAKAMI, T. DEGUCHI and A. MORITA, *J. Amer. Ceram. Soc.* **72** (1989) 1465.
5. P. DE LIMA NETO, M. ATIK, L. A. AUACA and M. A. AEGERTER, *J. Sol-Gel Sci. Technol.* **2** (1994) 529.

6. R. M. SHANE and M. L. MECARTNEY, *J. Mater. Sci.* **25** (1990) 1537.
7. P. PESHEV and V. SLAVOVA, *Mater. Res. Bull.* **27** (1992) 1269.
8. K. MIYAZAWA, K. SUZUKI and M. Y. WEY, *J. Amer. Ceram. Soc.* **78** (1995) 347.
9. M. YASHIMA, Y. MATSUO and M. YOSHIMURA, *J. Mater. Res.* **12** (1997) 2575.
10. C. H. CHANG, R. GOPALAN and Y. S. LIN, *J. Membr. Sci.* **91** (1994) 27.
11. R. GOPALAN, C. H. CHANG and Y. S. LIN, *J. Mater. Sci.* **30** (1995) 3075.
12. T. L. WEN, V. HERBERT and S. VILMINOT, *ibid.* **26** (1991) 3787.
13. P. PESHEV and V. SLAVOVA, *Mater. Res. Bull.* **27** (1992) 1269.
14. T. W. KUEPER, S. J. VISCO and L. C. DE JONGHE, *Solid State Ionics* **52** (1992) 251.
15. C. SAKURAI, T. FUZUKI and M. OKUYAMA, *J. Amer. Ceram. Soc.* **76** (1993) 1061.
16. W. D. KINGERY, H. K. BOWEN and D. R. UHLMANN, "Introduction to Ceramics" (Wiley, New York, 1976).
17. C. J. BRINKER and G. W. SCHERER, "Sol-Gel Science" (Academic Press, Boston, 1990).
18. S. RAMANATHAN, R. V. MURALEEDHARAN, S. K. ROY and P. K. NAYAR. *J. Amer. Ceram. Soc.* **78** (1995) 429.
19. R. C. GARVIE, *J. Phys. Chem.* **69** (1965) 1238.
20. R. P. INGEL and D. LEWIS III, *J. Amer. Ceram. Soc.* **69** (1986) 325.
21. C. H. PERRY, F. LU and B. ALZYAB, *J. Raman Spectroscopy* **21** (1990) 577.
22. T. HIRATA, *J. Phys. Chem. Solids* **7** (1995) 951.
23. C. J. HOWARD, R. J. HILL and B. E. REICHERT, *Acta Crystallogr.* **B44** (1988) 116.
24. J. M. LEGES, P. E. TOMASZEWSKI and A. S. PEREIRA, *Phys. Rev.* **B47** (1993) 14075.
25. D. R. CLARKE and E. ADAR, *J. Amer. Ceram. Soc.* **65** (1982) 284.
26. K. TSUKUMA and M. SHIMADA, *J. Mater. Sci.* **20** (1985) 1178.

Received 9 September 1998
and accepted 29 January 1999